

 Open access • Journal Article • DOI:10.1109/JLT.2020.2971666

Room-Temperature Power-Stabilized Narrow-Linewidth Tunable Erbium-Doped Fiber Ring Laser Based on Cascaded Mach-Zehnder Interferometers With Different Free Spectral Range for Strain Sensing — [Source link](#)

[Liqiang Zhang](#), [Zhen Tian](#), [Nan-Kuang Chen](#), [Haili Han](#) ...+6 more authors

Institutions: [Liaocheng University](#), [National Chung Hsing University](#), [University of London](#), [National Taiwan University of Science and Technology](#)

Published on: 01 Apr 2020 - [Journal of Lightwave Technology](#) (IEEE)

Topics: [Laser linewidth](#), [Fiber laser](#), [Tunable laser](#), [Lasing threshold](#) and [Extinction ratio](#)

Related papers:

- [Multi-wavelength tunable ring cavity fiber laser incorporated with a Mach–Zehnder interferometer filter based on waist-enlarged fiber bitapers](#)
- [Narrow spectral linewidth and tunable erbium-doped fiber ring laser using a MZI based on CHCF](#)
- [Tunable fiber laser based on a cascaded structure consisting of in-line MZI and traditional MZI](#)
- [Stable and widely tunable single-/dual-wavelength erbium-doped fiber laser by cascading a twin-core photonic crystal fiber based filter with Mach-Zehnder interferometer](#)
- [Large dynamic range operation of ultra-higher number MWFLs affected by MZI-SI](#)

Share this paper:    

View more about this paper here: <https://typeset.io/papers/room-temperature-power-stabilized-narrow-linewidth-tunable-4ghx9sm3t1>



City Research Online

City, University of London Institutional Repository

Citation: Zhang, L., Tian, Z., Chen, N-K., Han, H. K., Liu, C., Grattan, K. T. V. ORCID: 0000-0003-2250-3832, Rahman, B. M. ORCID: 0000-0001-6384-0961, Zhou, H., Liaw, S. K. and Bai, C. (2020). Room-Temperature Power-Stabilized Narrow-Linewidth Tunable Erbium-Doped Fiber Ring Laser Based on Cascaded Mach-Zehnder Interferometers with Different Free Spectral Range for Strain Sensing. *Journal of Lightwave Technology*, 38(7), pp. 1966-1974. doi: 10.1109/JLT.2020.2971666

This is the accepted version of the paper.

This version of the publication may differ from the final published version.

Permanent repository link: <https://openaccess.city.ac.uk/id/eprint/24150/>

Link to published version: <http://dx.doi.org/10.1109/JLT.2020.2971666>

Copyright: City Research Online aims to make research outputs of City, University of London available to a wider audience. Copyright and Moral Rights remain with the author(s) and/or copyright holders. URLs from City Research Online may be freely distributed and linked to.










Reuse: Copies of full items can be used for personal research or study, educational, or not-for-profit purposes without prior permission or charge. Provided that the authors, title and full bibliographic details are credited, a hyperlink and/or URL is given for the original metadata page and the content is not changed in any way.

City Research Online:

<http://openaccess.city.ac.uk/>

publications@city.ac.uk

Room-Temperature Power-Stabilized Narrow-Linewidth Tunable Erbium-Doped Fiber Ring Laser Based on Cascaded Mach-Zehnder Interferometers With Different Free Spectral Range for Strain Sensing

Liqiang Zhang , Zhen Tian , Nan-Kuang Chen , Haili Han , Chun-Nien Liu , Kenneth T. V. Grattan, B. M. A. Rahman , *Fellow, IEEE, Fellow, OSA*, Haimiao Zhou , Shien-Kuei Liaw , *Senior Member, IEEE, Senior Member, OSA*, and Chenglin Bai 

Abstract—An automatically power-stabilized (with power fluctuation <0.155 dB), narrow-linewidth (0.0171 nm), wavelength-tunable (10.69 nm) erbium-doped fiber laser has been proposed by cascading two fiber Mach-Zehnder interferometers (MZI) without using any temperature controlling device. One of the MZIs (here called the 1st MZI) is composed of two 3 dB couplers to form interference patterns while the other MZI (here termed the 2nd MZI) is constructed with a tapered seven-core fiber (SCF) and based on the principle of supermode interference. For the two MZIs, the free spectral range (FSR), the passband bandwidth and the extinction ratio (ER) at 1560 nm are 0.37 nm, 0.19 nm, 16.6 dB and 13.93 nm, 7.93 nm, 10.1 dB, respectively. Due to the major difference between the two FSR values, the 1st MZI and the 2nd MZI respectively play a role in controlling the laser linewidth and suppressing the homogeneous broadening effect to reach to a satisfactory level of power stability. The 2nd MZI is also used to fine tune the laser wavelength by applying strain to the tapered SCF (TSCF) over the spectral range of 1570.22–1559.33 nm, with an incremental step of 0.37 nm being used. The side-mode suppression ratio (SMSR) of the tunable fiber laser can be up to 45 dB. By appropriately adjusting the polarization controller, dual wavelength lasing can also be achieved.

This work was supported in part by the National Natural Science Foundation of China (NSFC) under Grant 61875247 and in part by the Liaocheng University under Grant 31805180101 and Grant 319190301. The support of the Royal Academy of Engineering is greatly appreciated.

L. Zhang, Z. Tian, N.-K. Chen, H. Han, H. Zhou, and C. Bai are with the School of Physics Sciences and Information Technology, and Key Laboratory of Optical Communication Science and Technology, Shandong Province, Liaocheng University, Liaocheng 252059, China (e-mail: zhangliqiang@lcu.edu.cn; tianzhen@lcu.edu.cn; nankuang@gmail.com; 1625946170@qq.com; 1170015139@qq.com; baichenglin@lcu.edu.cn).

C.-N. Liu is with the Department of Electrical Engineering, National Chung Hsing University, Taichung 402, Taiwan (e-mail: terbovine@gmail.com).

K. T. V. Grattan and B. M. A. Rahman are with the Department of Electrical and Electronic Engineering, University of London EC1V 0HB, London, United Kingdom (e-mail: K.T.V.Grattan@city.ac.uk; B.M.A.Rahman@city.ac.uk).

S.-K. Liaw is with the Graduate Institute of Electro-Optical Engineering, National Taiwan University of Science and Technology, Taipei 106, Taiwan (e-mail: skliaw@mail.ntust.edu.tw).

For single wavelength lasing, the 3 dB laser linewidth is 0.0171 nm. The power fluctuation, without a temperature controlling device being used and operating at room temperature, is found to be less than 0.155 dB over 1 hour while the central wavelength drift is less than 0.19 nm.

Index Terms—Erbium fiber laser, Mach-Zehnder interferometer, narrow linewidth, ring cavity, strain sensor, tunable laser.

I. INTRODUCTION

WITH the advent of various rare-earth-ion doped silica optical fibers and high power single-mode diode lasers, fiber lasers with many excellent optical characteristics such as high quantum efficiency, high gain bandwidth, high SMSR, high polarization extinction ratio, high output power, high pulse energy, low threshold pump power, wide tuning range and ultra-narrow linewidth have been developed extensively for applications in the field of communications, sensing, imaging, and micro- or nano-machining [1]–[3]. Further, practical applications of tunable erbium-doped fiber lasers (EDFL) include laser ranging, optical coherence tomography, wavelength division multiplexing and biosensing [4]–[7]. The wavelength tuning can usually be achieved using volume/fiber Bragg gratings (FBG) [8], [9], fiber filters, interferometers [10], [11] or indeed through many other methods [12]–[14]. The laser tuning range, linewidth, SMSR, and power stability are usually determined by the tuning devices used, such as a Mach-Zehnder interferometer (MZI) incorporated into the cavity. A wide and flat gain bandwidth, the inversion rate, and homogeneous broadening linewidth of the gain medium are also well known as important factors. It is known that the gain profile of the erbium-doped fiber (EDF) changes with the inversion rate. A lower inversion rate in the EDF is helpful to obtain a flatter gain plateau near 1550 nm, though the gain peak may enter the L-band (1560–1620 nm) regime. However, compared with C-band, the temperature stability is naturally a matter for both L-band and S-band amplification in EDF causing poor noise figures and more serious power fluctuation due to the Boltzman distribution

of the electrons occupying the excited states [15]. Moreover, the homogeneous broadening linewidth, naturally determined by the energy sublevels of the EDF, is also crucial to the power stability and the wavelength fluctuation: again the L-band is in its worst condition due to its greater broadening linewidth of 4–5 nm [16]. Consequently, with the use of suitable narrowband tunable fiber filters in the EDFL then operating under the proper inversion rate and spectral range, this is advantageous for achieving an EDFL with the desired lasing wavelengths, laser linewidth, SMSR, tuning range, and good environmental stability for accurate sensing applications. There have been several methods proposed using MZIs, FBGs, long-period gratings or Fabry-Perot interferometers to achieve multiwavelength lasing in an EDF [17]–[22]. However, the power fluctuation and the measured time period for the power stability to be achieved are usually much larger than 0.2 dB and less than 30 minutes, respectively [10], [18], [19].

In contrast in this work, two cascaded MZIs with very different FSR are employed in a ring cavity EDFL. The 1st MZI is composed of two 3 dB fiber couplers and a phase shifter to provide a comb-like spectral filtering with an FSR of 0.37 nm and a narrow passband bandwidth (PBW) of 0.19 nm. The 2nd MZI is comprised of a TSCF with a FSR of 13.93 nm and a PBW of 7.93 nm based on the interference of two supermodes. In the SCF, the six Ge-doped silica cores are evenly distributed and surrounding the central core with a rotational symmetry of 60°. The cores are well separated to avoid evanescent power coupling and therefore the optical characteristics are more like the weakly coupled SCF and no interference effects are produced [23]. However, when the SCF is heated and tapered by using a flame until the tapered diameter is below 35 μm , all the separated cores come closer to each other: the device becomes a strongly coupled SCF structure and the supermodes are thus excited to generate interference effects. The interferences caused by the two supermodes are sensitive to ambient variations of strain, bending, twist and so on. This TSCF serves as the 2nd MZI to provide an FSR which is wider than that of the 1st MZI. In addition, a tensile strain is also applied to the TSCF by mechanically stretching it to fine tune the lasing wavelength of the EDFL when these two MZIs are incorporated into a ring cavity. By correctly adjusting the polarization controller (PC), dual wavelength lasing can occur somewhere inside the interval spanning from the short wavelength border (1562.75 nm, 1562.4 nm) to the long wavelength border (1569.66 nm, 1569.25 nm). The purpose of using two cascaded MZIs is to achieve a narrow laser linewidth and simultaneously stabilize the output power. Accordingly, a power-stabilized wavelength-tunable single/dual wavelength EDFL operating at room temperature is achieved. The laser linewidth, SMSR and tuning range, are 0.0178 nm, 45 dB, 10.69 nm (1570.22–1559.33 nm), respectively. The power fluctuation of the 974 nm pump laser is 0.02 dB over a period of an hour and under this situation the output power fluctuation of the EDFL is 0.155 dB (over an hour at room temperature) without any temperature controlling device used. The corresponding central wavelength drift is less than 0.19 nm and the strain sensitivity is 0.0525 nm/ μE . The results achieved here are generally better than most of the previous reports for EDFLs in the literature [17]–[22]. The room-temperature power-stabilized, narrow-linewidth, single-/dual-wavelength

switchable, wavelength-tunable EDFL with high SMSR and high strain sensitivity based on two cascaded MZIs with different FSR thus developed is useful for sensing, imaging, communications, and micromachining systems, offering high accuracy.

II. WORKING PRINCIPLE AND EXPERIMENTAL SET-UP

The laser cavity of the EDFL can be usually categorized as either a linear or ring cavity [8]–[10]. The ring cavity featured here is a simple structure without using reflective elements and efficient pumping is achieved by recycling the residual pump radiation. The experimental set-up for the EDFL is shown in Fig. 1(a) in which a 10-m-long C-band EDF is used and the gain spectra under 974 nm pumping, at different inversion rates, is shown in Fig. 1(b). Clearly, the optical gain increases with increasing pump power while the gain peak gradually moves toward 1530 nm, from 1570 nm. A lower inversion rate can lead to a flatter gain plateau near 1550 nm, to help widen the wavelength tuning range for the EDFL. However, the ASE will not be substantially suppressed and to achieve sufficient gain with a higher SMSR and a wider tuning range, the wavelength of 974 nm for the pump, at a power of 41.8 mW is selected. In order to suppress the backward propagating amplified spontaneous emission (ASE) and enhance the SMSR in the EDFL, an isolator (ISO) is used in the ring cavity, to achieve unidirectional lasing. The PC is used to improve the output power and the polarization extinction ratio. The intra-cavity filters used in this work for wavelength-selection are two cascaded fiber MZIs with different FSR. The 1st MZI is composed of two broadband 3 dB fiber couplers (with a total bilateral leading fiber length of about 2 m) and a phase shifter, as shown schematically in Fig. 1(a). The 3 dB couplers are used for power splitting and combing, respectively. The phase shifter is formed by using two physically separated optical fibers with a length difference of 1.6 mm, to generate comb-like filtering. The FSR, PBW, and ER at 1560 nm are 0.37 nm, 0.19 nm, and 16.6 dB, respectively and the transmission spectrum is shown in Fig. 1(c). The main purpose of using the 1st MZI is to achieve narrow linewidth lasing in the EDFL. The 2nd MZI, sample A, comprises an 8-mm-long TSCF in a 5-cm-long SCF, splicing between two single mode fibers (SMF) to provide the filtered spectrum shown in Fig. 1(d). Its corresponding FSR, PBW and ER at 1560 nm are 13.93 nm, 7.93 nm, and 10.1 dB, respectively. The 2nd MZI is used for suppressing the influence of homogenous broadening and for fine tuning the lasing wavelength when a tensile force is applied. By cascading the 1st and the 2nd MZIs in a ring laser cavity, the total transfer function for the filtering yields the spectrum shown in Fig. 1(e) in which the periodic oscillations in Fig. 1(c) are thus modulated by the 2nd MZI. For this EDFL, no temperature compensating or other controlling device is used.

The SCF is originally designed to enlarge the transmission capacity by space division multiplexing when each of the seven cores independently transmit signals along the fiber. The cross-sectional micrograph of the SCF with a tapered diameter, D , of 8.2 μm and operating at 1550 nm. For the SCF, the six Ge-doped cores are evenly distributed and surrounding the central core and the spacing between each core is 29 μm (to avoid evanescent power coupling). The core diameter and the numerical aperture

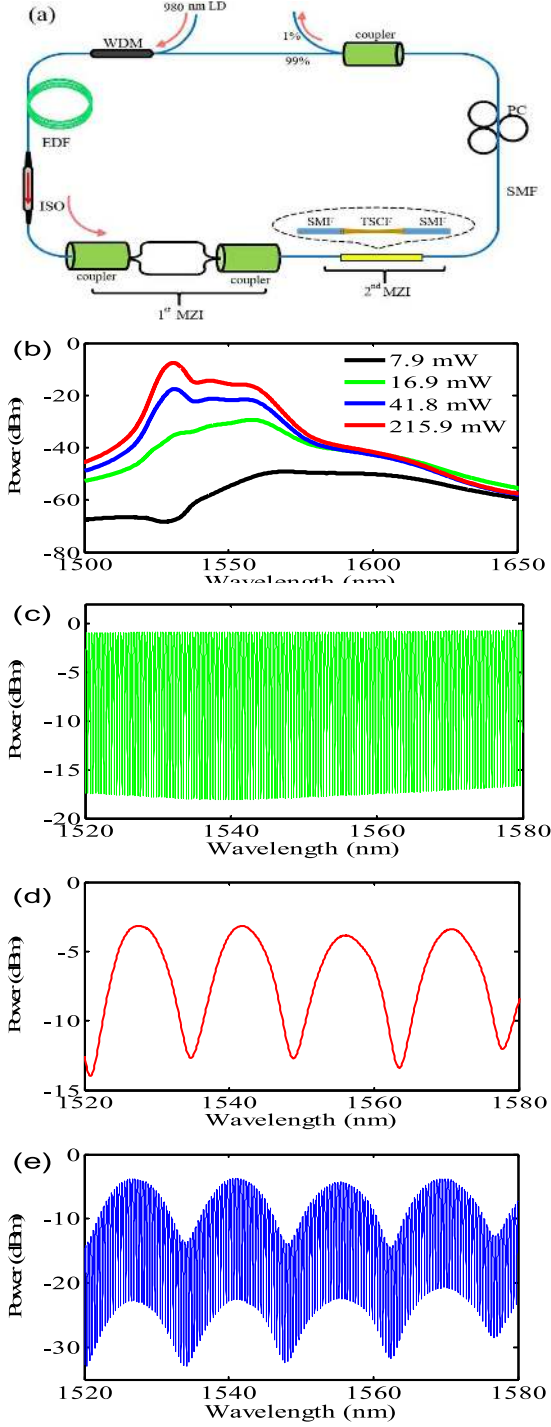


Fig. 1. (a) Experimental set-up of the EDFL used. TSCF: tapered seven-core fiber, LD: laser diode, WDM: wavelength division multiplexer, ISO: isolator, PC: polarization controller. (b) Gain profile of EDF at different pump power. Measured transmission spectra for (c) 1st MZI, (d) 2nd MZI, and (e) cascaded MZIs.

(NA) for each core are $5.62 \mu\text{m}$ and 0.2 , respectively. To avoid exciting the high order core modes, two special SMFs with a NA of 0.15 and 0.2 are inserted (in that order) between the standard SMF (NA = 0.13) and the SCF, achieving a NA transition by fusion splicing. Moreover, the SCF near the splicing point is

also intentionally coiled with a radius of curvature of 5 mm to suppress significantly the excitation of the high order modes.

As mentioned above, the 2nd MZI is made by splicing a segment of SCF between two SMFs. When a part of the SCF is tapered, the core diameter and the spacing between adjacent cores are both reduced to turn this TSCF into a strongly coupled MCF. This produces the intermodal coupling and the supermodes are thus excited to generate interferences in the TSCF. To analyze the operating principle of the supermodes interference in the TSCF, a coupled mode equation is employed. When the light is launched into the central core of the TSCF, the coupled equation can be written as [24],

$$\frac{d\vec{A}}{dz} = -\vec{C}\vec{A}(z), \quad (1)$$

where $\vec{A} = [A_1(z)A_2(z)A_3(z)A_4(z)A_5(z)A_6(z)A_7(z)]^T$ is the column vector of the amplitude of each core mode of the tapered SCF. \vec{C} is a matrix of the coupling coefficient, and the elements c_{pq} can be written as

$$c_{pq} = \begin{cases} jC_{pq} \exp[j(\beta_p - \beta_q)z], & p \neq q \\ 0, & p = q \end{cases}, \quad (2)$$

where β_p represents the propagation constant of core mode p . For the homogenous SCF, the propagation constants for each core mode should be the same, and C is thus given as follows:

$$\vec{C} = \begin{pmatrix} 0 & C & C & C & C & C & C \\ C & 0 & C & 0 & 0 & 0 & C \\ C & C & 0 & C & 0 & 0 & 0 \\ C & 0 & C & 0 & C & 0 & 0 \\ C & 0 & 0 & C & 0 & C & 0 \\ C & 0 & 0 & 0 & C & 0 & C \\ C & C & 0 & 0 & 0 & C & 0 \end{pmatrix}, \quad (3)$$

where the off-diagonal zeros correspond to the pairs of cores, assumed that the coupling between cores are negligible due to the large inter-core distances. If the light is launched into the central core, the intensities of the normalized central core mode and the six side-core modes can be derived as

$$|A_1(z)|^2 = \frac{1}{7} + \frac{6}{7} \cos^2(\sqrt{7}Cz) \quad (4)$$

$$|A_p(z)|^2 = \frac{1}{7} \sin^2(\sqrt{7}Cz) \quad p \neq 1 \quad (5)$$

The coupling coefficient C can be derived as [25], [26]

$$C = \frac{\pi}{2} \frac{\sqrt{n_1^2 - n_2^2} U^2}{an_1} \frac{K_0(Wd/a)}{V^2 K_1^2(W)}, \quad (6)$$

where n_1 and n_2 are the refractive indices of the core and cladding modes, respectively. a and d are the core diameter and the distance between two cores, respectively. K_0 and K_1 represent the 0 and the 1st order Henkel functions. U , W and V are respectively the normalized radial phase constant, normalized radial attenuation constant, and the normalized

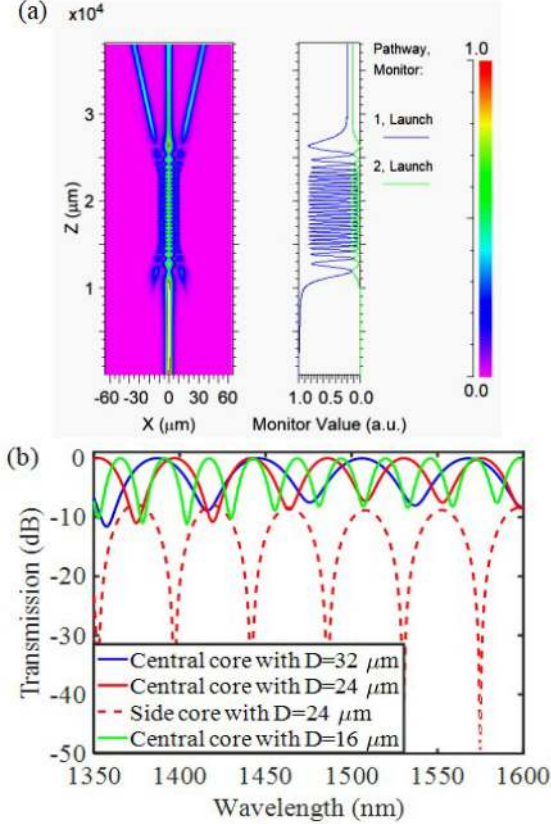


Fig. 2. Simulation results using a Rsoft software. (a) Propagation field distribution and the normalized propagating power along the TSCF at 1550 nm. (b) Transmission spectra of the TSCF.

frequency and they are defined as

$$U = a\sqrt{(2\pi n_1/\lambda)^2 - \beta^2}, \quad V = \frac{2\pi a}{\lambda} \sqrt{n_1^2 - n_2^2},$$

$$W = a\sqrt{\beta^2 - (2\pi n_2/\lambda)^2}. \quad (7)$$

From Eqs. (4) and (5), it is evident that the central core mode and the side core modes can be beat periodically with a phase difference of $\pi/2$ [24]. The variation of the tapered fiber diameter changes the core diameter and the spacing between two cores, resulting in the variation of the coupling strength among multiple cores. The structure was simulated using a beam propagation method (BPM) module from Rsoft 2019 software to analyze the light propagating through the TSCF. The effective refractive indices of the core and cladding are 1.459 and 1.444 respectively at 1550 nm wavelength. The core diameter and the distance between each core are set to be $5.62 \mu\text{m}$ and $29 \mu\text{m}$, respectively. The length of the uniform tapered region is 8 mm. The results are shown in Fig. 2(a). Fig. 2(a) gives the propagation and the normalized propagating power along the TSCF at the input wavelength of 1550 nm when the tapered diameter is $24 \mu\text{m}$. The input light is launched into the central core. As shown in Fig. 2(a), it is apparent that the light is tightly confined in the central core before the SCF is tapered. In the tapered region, the distance between each core is reduced and the evanescent field of the core mode is extended simultaneously. Thus, intermodal

coupling between the central core mode and side core modes is induced. When the light is passing through the tapered region, the field is divided to propagate in central core and side cores. Fig. 2(b) shows the calculated transmission spectra of central core mode for the TSCF at a D of $32 \mu\text{m}$ (blue solid line), $24 \mu\text{m}$ (red solid line) and $16 \mu\text{m}$ (green solid line), respectively. The FSR decrease with a decreasing D . To investigate the phase difference between central core mode and side core mode, the transmission spectra of one of the side core mode (red dashed line) is also given in Fig. 2(b) with the tapered diameter of $24 \mu\text{m}$. The phase difference of the transmission oscillations of the central core (red solid line) and side core mode (red dashed line) was estimated to be $\pi/2$, which agrees with the results shown in Eqs. (4) and (5).

To investigate the optical characteristics of the TSCF interferometer, it is found that when the SCF is tapered until D is below $60 \mu\text{m}$, the supermodes can be excited since the seven cores come closer to become a strongly coupled waveguide structure [27]. The typical mode field patterns, taken using a $1000\times$ CCD microscope, of the SCF and the supermode in TSCF, for the case where D is $60 \mu\text{m}$, are shown in Fig. 3(a) and 3(b), respectively. The supermodes interfere with each other and thus produce interference effects [27]. When the broadband spectrum (spanning the wavelength range 1250- 1650 nm) from the superluminescent diodes is launched into the central core of the SCF, the transmission spectra for the TSCF at different values of D ($24 \mu\text{m}$, $13 \mu\text{m}$, and $7 \mu\text{m}$) are respectively shown in Fig. 3(c)–(e). In agreements with the results of the simulations, the FSR and ER respectively decrease and increase with decreasing value of D . From Fig. 3(d), the best value of ER achieved can be up to 27.9 dB, at 1504.3 nm. The temperature sensitivity of the 2nd MZI is also investigated using another TSCF, sample B, with D of $8.12 \mu\text{m}$, and the results are shown in Fig. 4. When the temperature was increased from $20 \text{ }^\circ\text{C}$ to $80 \text{ }^\circ\text{C}$. One of the dip wavelengths observed drifts from 1555.92 nm to 1556.64 nm. Consequently, the temperature sensitivity is $11.5 \text{ pm}/^\circ\text{C}$ which is small enough to allow the EDFL to operate in a very stable manner.

By applying a tensile strain to the two ends of the TSCF using stepping motors, the spectral responses of the cascaded MZIs are shown in Fig. 5, with a gradually increasing step of $45 \mu\text{m}$ from top to bottom. The FSR and PBW seen for fast oscillations are unchanged, whereas the FSR for the slowly varying envelope varies slightly with changing tensile force. By monitoring a particular peak wavelength of the envelope, at 1559.11 nm, the wavelength red-shifts with increasing values of applied strain. As a result, the lasing wavelength can be tuned by varying the strain and dual wavelength lasing can also be generated by appropriately adjusting the PC. Eventually, a TSCF with a value of $D = 8.2 \mu\text{m}$ is inserted into the ring cavity of the EDFL, to be used as the 2nd MZI, for measurement purposes.

III. RESULTS AND DISCUSSIONS

In the experiment carried out, a 974 nm wavelength-locked laser diode (LD) with 400 mW maximum output power is used as the pump source. The pump power fluctuation is 0.02 dB

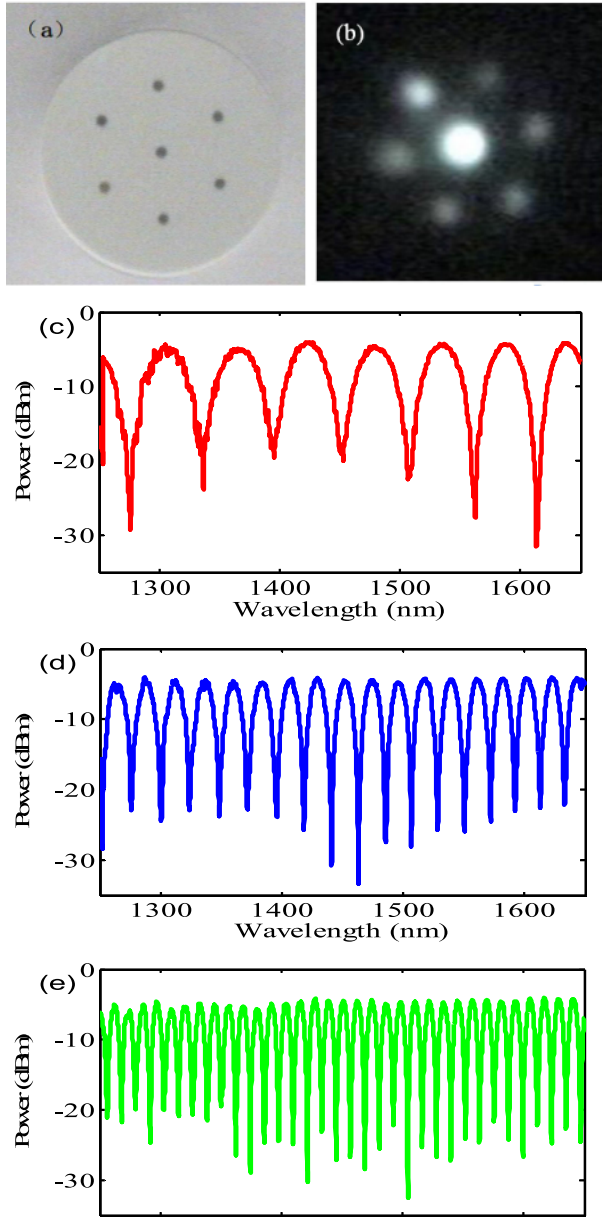


Fig. 3. Cross-sectional micrograph of (a) SCF and (b) the mode field pattern of TSCF. The measured transmission spectra of the TSCF at different values of D of (b) $24 \mu\text{m}$, (c) $13 \mu\text{m}$, and (d) $7 \mu\text{m}$.

in an hour at room temperature. The pump light is launched into the 10-m-long EDF through a 980/1550 nm WDM coupler and an output coupler (OC) is used to tap 1% optical power from ring cavity as laser output. The spectral responses for different pump powers, shown in Fig. 6, are recorded by using an Optical Spectrum Analyzer (OSA, Yokogawa, AQ6370D) with an optical resolution of 0.02 nm. The threshold pump power of the EDFL is 7.9 mW and the initial lasing occurs at 1564.06 nm. By continuously increasing the pump power, P , the SMSR was gradually increased to a maximum of 45 dB, with a laser linewidth of 0.0171 nm until $P = 41.8$ mW is reached, as shown in Fig. 7. The initial lasing wavelength changed to 1563.96 nm when P was increased to 16.9 mW. This arises because at the initial stage, a higher inversion rate makes

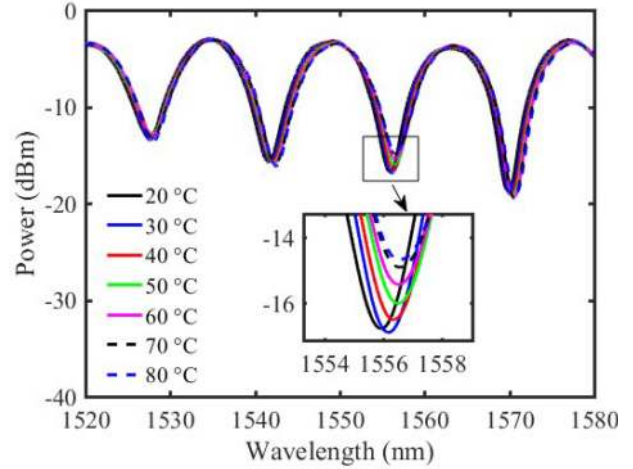


Fig. 4. Temperature sensitivity of the second MZI.

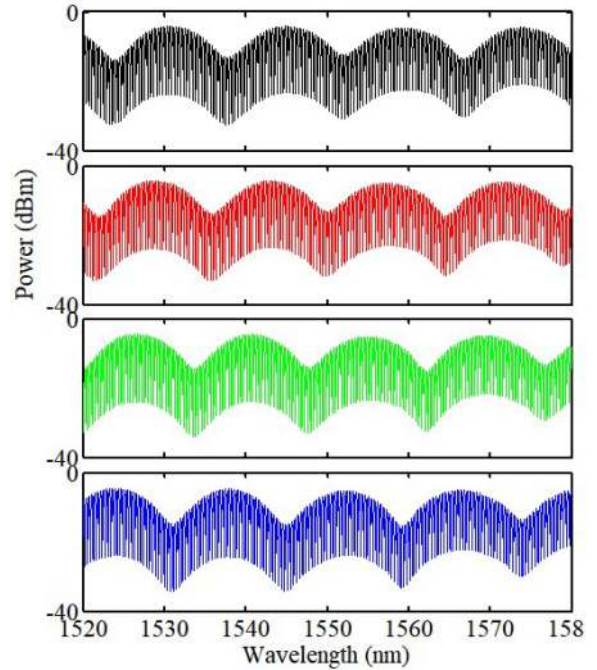


Fig. 5. Spectral responses of the cascaded MZIs varying with different strain values, with an increment of $45 \mu\epsilon$.

the gain peak substantially blue-shift and the gain coefficient increases, as can be seen in Fig. 1(b). The gain peak for $P = 16.9$ mW is located at 1563.96 nm. For the situations where P is above 16.9 mW, the lasing wavelength is almost stabilized at 1563.96 nm. When the value of P goes beyond 41.8 mW, the laser output power reaches a maximum of -20 dBm and other multiple lasing wavelengths start to grow on both sides of 1563.96 nm. In the case multiple wavelength lasing, the FSR is 0.37 nm, which is mainly determined by the 1st MZI and remains the same at different values of P . The 10-m-long EDF is fully inverted when P is 219.5 mW. The central lasing wavelength does not move with increasing value of P and multiple wavelength lasing can be produced simultaneously when P is

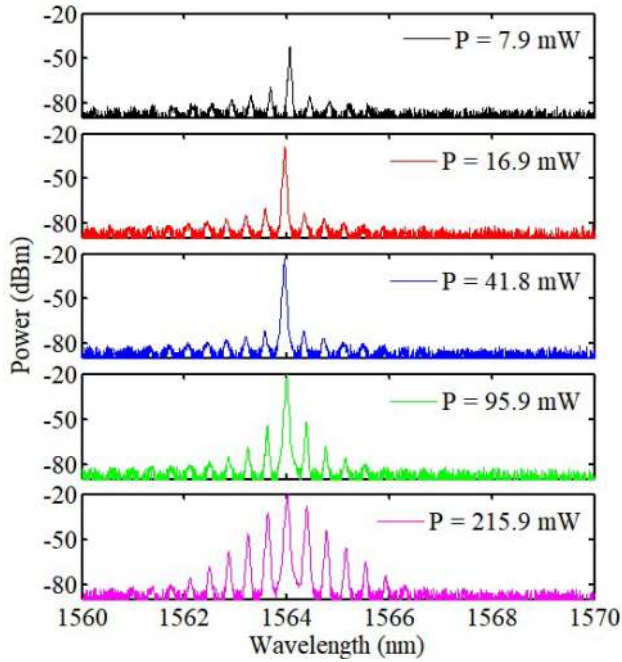


Fig. 6. Spectra of the fiber laser at different pump

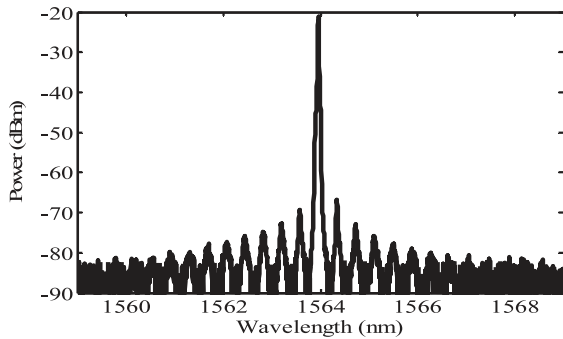


Fig. 7. Spectrum of the EDFL when P is 41.8 mW.

above 16.9 mW. This arises because of the existence of the 1st and 2nd MZI having greatly suppressed the influence of the homogeneous broadening effect, even if the gain peak for the EDF blue-shifts, to 1531 nm, when P is set to 41.8 mW.

To achieve wavelength fine tuning, when P is fixed at 41.8 mW, a tensile strain is applied to the 2nd MZI: here the two ends of TSCF are fixed by clamps mounted on a stepper motor (with a spatial resolution of $1 \mu\text{m}$). The lasing wavelength gradually red-shifts with increasing strain, with an increment of $19 \mu\text{E}$ used. When the elongation of the TSCF increases from $16 \mu\text{m}$ to $39 \mu\text{m}$, the lasing wavelength can be tuned from 1570.22 nm to 1559.33 nm with a corresponding tuning range of 10.69 nm. The SMSR for all the lasing conditions is always higher than 40 dB. By further elongating the TSCF, the lasing wavelength jumps back to 1570.07 nm, as shown in Fig. 8(a). Again, this shows explicitly that the 1st and 2nd MZI respectively determine the laser linewidth and suppress the optical gain outside the 1560–1570 nm range. The position of the 1st and the 2nd MZI has also been exchanged and no obvious changes can be observed,

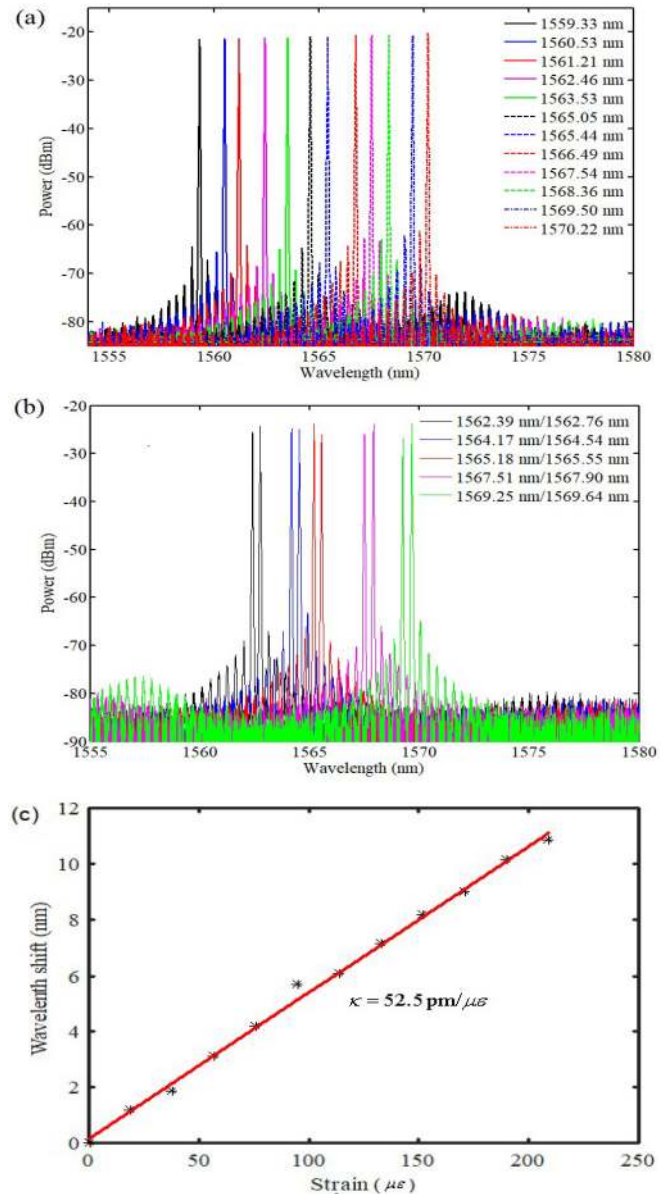


Fig. 8. Spectral responses of the EDFL for (a) single wavelength lasing and tuning by strain and (b) dual wavelength lasing and tuning and (c) wavelength shift versus applied strain, sample A.

as the overall system is reciprocal. By changing the state of polarization through a PC, dual-wavelength lasing can thus be achieved, as shown in Fig. 8(b). These dual lasing wavelengths occurs somewhere inside the interval from the short wavelength border (1562.75 nm, 1562.4 nm) to the long wavelength border (1569.66 nm, 1569.25 nm), this being contingent upon the state of polarization. The FSR between the dual lasing wavelengths is 0.37 nm under all these conditions, which is in agreement with the FSR of the 1st MZI. For single wavelength lasing, this tunable EDFL can also be used as a strain sensor by monitoring the wavelength shift achieved. The corresponding results of the relationship between the wavelength shift and applied strain are shown in Fig. 8(c), yielding a strain sensitivity of $52.5 \text{ pm}/\mu\text{E}$ - this result is more accurate than seen in some previous reports in

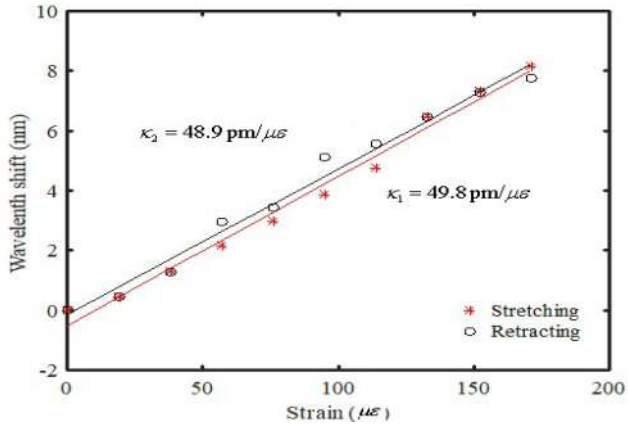


Fig. 9. Wavelength shift versus applied tensile strain for the TSCF, sample B, under the stretching and retracting situations.

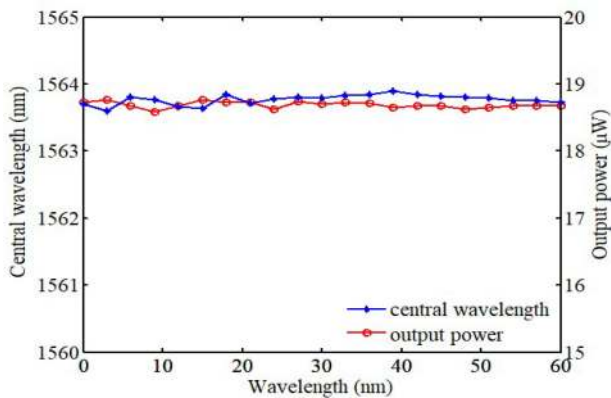


Fig. 10. Central wavelength drift and output power stability of EDFL at room temperature over a period of an hour.

the literature [28]–[30]. To investigate the reproducibility of the wavelength shift under different tensile strain for the TSCF, the sample B was used and the relationship between the wavelength shifts and applied strain at an increment of $2 \mu\text{m}$ are shown in Fig. 9. From Fig. 9, the strain sensitivity κ_1 and κ_2 for the stretching and retracting are $49.8 \text{ pm}/\mu\text{ε}$ and $48.9 \text{ pm}/\mu\text{ε}$, respectively. Obviously, the reproducibility for the TSCF is quite good and this is advantageous to make tunable EDFL with desired lasing wavelengths.

To investigate the stability of the EDFL at room temperature, monitoring of the central wavelength drift and output power stability for single wavelength lasing were both done over a period of an hour and the results are shown in Fig. 10. The OSA was set-up to scan repeatedly (every 5 minutes for an hour in total). During this hour of monitoring, the EDFL was placed on a smart optical table (Newport: RS 2000) and no part of the laser system was adjusted or moved. In Fig. 10, the measured central wavelength drift and the power fluctuation observed are respectively less than 0.19 nm and 0.155 dB . In contrast to previous reports in the literature on the stability of fiber lasers, the performance of the EDFL using a cascaded MZIs

TABLE I
PARAMETERS FOR EDFLS: COMPARISON OF THIS WORK
WITH LITERATURE DATA

	power fluctuation	period of time	tuning range	laser linewidth	SMSR	wavelength drift
current work	0.155 dB*	1 hour	10.69 nm	0.0171 nm	45 dB	0.19 nm
Ref. 5	0.2 dB	NA	NA	NA	40 dB	0.1 nm
Ref. 10	1.0 dB	30 min	NA	NA	NA	0.05 nm
Ref. 11	1 dB	30 min	0.7 nm	0.012 nm	55 dB	NA
Ref. 17	0.84 dB	2 hours	NA	NA	NA	0.03 nm
Ref. 8	2 dB	30 min	3.4 nm	0.02 nm	50 dB	0.1 nm
Ref. 19	0.29 dB	20 min	22.2 nm	0.02 nm	36 dB	NA
Ref. 20	0.47 dB	2 hours	23.04 nm	0.026 nm	45 dB	0.02 nm
Ref. 21	0.82 dB	10 min	NA	0.03 nm	25.4 dB	NA
Ref. 22	NA	NA	50 nm	0.1 nm	45 dB	NA

*performance superior to all previous literature reports. NA: not available

with different FSRs in this work is superior, in terms of the power stability and monitoring time period used. The results are listed in Table I, with literature data for comparison. The central wavelength drift is still better than has been reported in most other works [17]–[22], although still not optimum. Consequently, the EDFL reported with two MZIs with different FSR can be automatically power-stabilized at room temperature, for an hour. The EDFL is also sensitive to strain on the 2nd MZI using TSCF and can also be employed as a strain sensing device (with its high accuracy ascribing to the power-stabilized EDFL).

IV. CONCLUSION

By cascading two MZIs with different FSRs, an EDFL with single-/dual wavelength lasing has been demonstrated. The 2nd MZI comprises a TSCF which is sensitive to tensile strain which then allows the achievement of wavelength tuning. The EDFL for single wavelength lasing was shown to be tunable over $1570.22\text{--}1559.33 \text{ nm}$ and the best SMSR achieved was 45 dB , with the laser linewidth being 0.0171 nm . The power fluctuation and central wavelength drift over a period of an hour were respectively less than 0.155 dB and 0.19 nm and the strain sensitivity κ achieved was $52.5 \text{ pm}/\mu\text{ε}$. This result is superior to most previous works reported and is believed to be due to the contribution from the 2nd MZI based supermode interference in the tapered seven-core fiber. This EDFL is automatically power-stabilized at room temperature, simple and single-/dual-wavelength lasing switchable and thus is promising for accurate strain sensing applications.

REFERENCES

- [1] L. G. Holmen *et al.*, “Tunable holmium-doped fiber laser with multi-watt operation from 2025 nm to 2200 nm ,” *Opt. Lett.*, vol. 44, no. 17, pp. 4131–4134, 2019.
- [2] H. W. Chen, H. T. Huang, S. Q. Wang, and D. Y. Shen, “A high-peak-power orthogonally-polarized multi-wavelength laser at $1.6\text{--}1.7 \mu\text{m}$ based on the cascaded nonlinear optical frequency conversion,” *Opt. Express*, vol. 27, no. 17, pp. 24857–24865, 2019.
- [3] T. C. Yin, Y. F. Song, X. G. Jiang, F. H. Chen, and S. L. He, “400 mW narrow linewidth single-frequency fiber ring cavity laser in $2 \mu\text{m}$ waveband,” *Opt. Express*, vol. 27, no. 11, pp. 15794–15799, 2019.

- [4] A. Castillo-Guzman, J. E. Antonio-Lopez, R. Selvas-Aguilar, D. A. May-Arrijoa, J. Estudillo-Ayala, and P. LiKamWa, "Widely tunable erbium-doped fiber laser based on multimode interference effect," *Opt. Express*, vol. 18, no. 2, pp. 591–597, 2010.
- [5] M. Yan, S. Y. Luo, L. Zhan, Z. M. Zhang, and Y. X. Xia, "Triple-wavelength switchable erbium-doped fiber laser with cascaded asymmetric exposure long-period fiber grating," *Opt. Express*, vol. 15, no. 7, pp. 3685–3691, 2007.
- [6] L. Zhang, J. M. Hu, J. H. Wang, and Y. Feng, "Tunable all-fiber dissipative-soliton laser with a multimode interference filter," *Opt. Lett.*, vol. 37, no. 18, pp. 3828–3830, 2012.
- [7] L. Ma, J. Sun, Y. H. Qi, Z. X. Kang, and S. S. Jian, "Switchable multi-wavelength fiber laser based on modal interference," *Chin. Phys. B*, vol. 24, no. 8, 2015, Art. no. 084201.
- [8] P. Zeil, V. Pasiskevicius, and F. Laurell, "Efficient spectral control and tuning of a high-power narrow-linewidth Yb-doped fiber laser using a transversely chirped volume Bragg grating," *Opt. Express*, vol. 21, no. 4, pp. 4027–4035, 2013.
- [9] F. Wang, D. Shen, D. Fan, and Q. Lu, "Spectrum narrowing of high power Tm: fiber laser using a volume Bragg grating," *Opt. Express*, vol. 18, no. 9, pp. 8937–8941, 2010.
- [10] A. P. Luo, Z. C. Luo, and W. C. Xu, "Tunable and switchable multi-wavelength erbium-doped fiber ring laser based on a modified dual-pass Mach-Zehnder interferometer," *Opt. Lett.*, vol. 34, no. 14, pp. 2135–2137, 2009.
- [11] S. C. Feng, S. H. Lu, W. J. Peng, Q. Li, T. Feng, and S. S. Jian, "Tunable single-polarization single-longitudinal-mode erbium-doped fiber ring laser employing a CMFBG filter and saturable absorber," *Opt. Laser Technol.*, vol. 47, pp. 102–106, 2013.
- [12] J. E. Antonio-Lopez, A. Castillo-Guzman, D. A. May-Arrijoa, R. Selvas-Aguilar, and P. Likam Wa, "Tunable multimode-interference bandpass fiber filter," *Opt. Lett.*, vol. 35, no. 3, pp. 324–326, 2010.
- [13] L. Ma, Y. H. Qi, Z. X. Kang, Y. L. Bai, and S. S. Jian, "Tunable fiber laser based on the refractive index characteristic of MMI effect," *Opt. Laser Technol.*, vol. 57, pp. 96–99, 2014.
- [14] T. Walbaum and C. Fallnich, "Multimode interference filter for tuning of a mode-locked all-fiber erbium laser," *Opt. Lett.*, vol. 36, no. 13, pp. 2459–2461, 2011.
- [15] N. K. Chen, C. M. Hung, S. Chi, and Y. Lai, "Towards the short-wavelength limit lasing at 1450 nm over 4I13/2 4I15/2 transition in silica-based erbium-doped fiber," *Opt. Express*, vol. 15, no. 25, pp. 16448–16456, 2007.
- [16] S. Sudo, *Optical Fiber Amplifiers: Materials, Devices, and Applications*. Artech House: Norwood, MA, USA 1997, Chap. 2.
- [17] J. Gutierrez-Gutierrez *et al.*, "Switchable and multi-wavelength linear fiber laser based on Fabry-Perot and Mach-Zehnder interferometers," *Opt. Commun.*, vol. 374, pp. 39–44, 2016.
- [18] T. L. Zhao, Z. G. Lian, X. Wang, Y. Shen, and S. Q. Lou, "Switchable and tunable erbium-doped fiber lasers using a hollow-core Bragg fiber," *Laser Phys. Lett.*, vol. 13, 2016, Art. no. 115104.
- [19] W. He, L. Q. Zhu, M. L. Dong, X. P. Lou, and F. Luo, "Wavelength-switchable and stable-ring-cavity, Erbium-doped fiber laser based on Mach-Zehnder interferometer and tunable filter," *Laser Phys.*, vol. 28, 2018, Art. no. 045104.
- [20] Z. J. Tang, S. Q. Lou, and X. Wang, "Stable and widely tunable single/dual-wavelength erbium-doped fiber laser by cascading a twin-core photonic crystal fiber based filter with Mach-Zehnder interferometer," *Opt. Laser Technol.*, vol. 109, pp. 249–255, 2019.
- [21] W. He, W. Zhang, L. Q. Zhu, X. P. Lou, and M. L. Dong, "C-band switchable multi-wavelength erbium-doped fiber laser based on Mach-Zehnder interferometer employing seven-core fiber," *Opt. Fiber Technol.*, vol. 46, pp. 30–35, 2018.
- [22] Y. W. Zhou and G. Y. Sun, "Widely tunable Erbium-doped fiber laser based on superimposed core-cladding-mode and Sagnac interferences," *IEEE Photon. J.*, vol. 4, no. 5, pp. 1504–1509, Oct. 2012.
- [23] G. Salceda-Delgado, A. Van Newkirk, J. E. Antonio-Lopez, A. Martinez-Rios, A. Schülzgen, and R. Amezcua Correa, "Compact fiber-optic curvature sensor based on super-mode interference in a seven-core fiber," *Opt. Lett.*, vol. 40, 7, pp. 1468–1471, 2015.
- [24] F. Y. M. Chan, A. P. T. Lau, and H. -Y. Tam, "Mode coupling dynamics and communication strategies for multi-core fiber systems," *Opt. Express*, vol. 20, no. 4, pp. 4548–4563, 2012.
- [25] M. -S. Yoon, S. -B. Lee, and Y. -G. Han, "In-line interferometer based on intermodal coupling of a multicore fiber," *Opt. Express*, vol. 23, no. 14, pp. 18316–18322, 2015.
- [26] A. W. Snyder, "Coupled-mode theory for optical fibers," *J. Opt. Soc. Am.*, vol. 62, no. 11, pp. 1267–1277, 1972.
- [27] J. Villatoro, O. Arrizabalaga, E. Antonio-Lopez, J. Zubia, and I. S. de Ocariz, "Multicore fiber sensors," in *Proc. Opt. Fiber Commun. Conf. Exhib.*, 2017, Art. no. Th3H.1.
- [28] K. Tian *et al.*, "Strain sensor based on gourd-shaped single-mode-multimode-single-mode hybrid optical fibre structure," *Opt. Express*, vol. 25, no. 16, pp. 18885–18896, 2017.
- [29] X. K. Bai, D. F. Fan, S. F. Wang, S. L. Pu, and X. L. Zeng, "Strain sensor based on fiber ring cavity laser with photonic crystal fiber in-line Mach-Zehnder interferometer," *IEEE Photon. J.*, vol. 6, no. 4, Aug. 2014, Art. no. 6801608.
- [30] C. R. Liao, D. N. Wang, and Y. Wang, "Microfiber in-line Mach-Zehnder interferometer for strain sensing," *Opt. Lett.*, vol. 38, no. 5, pp. 757–759, 2013.

Liqiang Zhang received the doctor of engineering degree in 2014 and is currently a Lecturer. Her research interests include advanced laser technology and application, nonlinear optics, and the related fields.

Zhen Tian is an Associate Professor. Her research interests focuses on mode-locked fiber lasers.

Nan-Kuang Chen has been invited to be a Ph. D. Student co-supervisor for IIT, Dhanbad, India, since September, 2016, SPIE (the international society for optics and photonics) Travelling Lecturer in 2015 and 2017. From 2018, he has been serving as a Distinguished Professor with the School of Physics Science and Information Technology, Liaocheng University, Liaocheng, China. His research interests include micro-/nano-fiber interferometric sensors, dispersion engineering technique, Cr³⁺-doped fiber amplifier, large core high power fiber lasers, and mode-locked femtosecond fiber lasers.

Haili Han is currently working toward the master's degree in the major of optical engineering with Liaocheng University, Liaocheng, China.

Chun-Nien Liu received the B.S. degree in physics from the National Changhua University of Education, Changhua, Taiwan, and the M.S. and Ph.D. degrees from the Department of Photonics, National Sun Yat-sen University, Kaohsiung, Taiwan, in 2010 and 2015, respectively. He received the Postdoctoral Research from the Graduate Institute of Optoelectronic Engineering, National Chung Hsing University, Taichung, Taiwan, in 2019 where he is currently an Assistant Professor with the Department of Electrical Engineering, National Chung Hsing University. His research interests include broadband Cr-doped fiber, specialty fiber, fiber microlens, near-field measurement of fiber coupling, package of laser module, and high-power LED based on glass host. He is a member of the OSA.

Kenneth T. V. Grattan received the B.Sc. degree (First Class Hons.) in physics from Queen's University, Belfast, U.K., in 1974, and the Ph.D degree in laser physics in 1979. He received the Doctor of Science degree from City University, London, U.K., in 1992 for his sensor work. His doctoral research involved the use of laser-probe techniques for measurements on potential new laser systems.

Following Queen's in 1978, he became a Research Fellow with the Imperial College of Science and Technology, sponsored by the Rutherford Laboratory to work on advanced photolytic drivers for novel laser systems. This involved detailed measurements of the characteristics and properties of novel laser species and a range of materials involved in systems calibration.

In 1983, he joined City University London as a "new blood" Lecturer in physics, being appointed a Professor of Measurement and Instrumentation in 1991 and the Head of the Department of Electrical, Electronic, and Information Engineering. From 2001 to 2008, he was an Associate and then Deputy Dean of the School of Engineering and from 2008 to 2012 the first Conjoint Dean of the School of Engineering & Mathematical Sciences and the School of Informatics. In 2013, he was appointed the Inaugural Dean of the City Graduate School. He was appointed the George Daniels Professor of Scientific Instrumentation in 2013 and to a Royal Academy of Engineering Research Chair in 2014. He is a Visiting Professor with several major Universities in China, with strong links to Harbin Engineering University and the Shandong Academy of Sciences. He is the author and co-author of more than seven hundred refereed publications in major international journals and at conferences and is the co-editor (with Professor B T Meggitt) of five volume topical series on Optical Fiber Sensor Technology. His work is highly cited by his peers nationally and internationally. His research interests have expanded to include the development and use of fibre optic and optical systems in the measurement of a range of physical and chemical parameters. The work has been sponsored by a number of organizations including EPSRC, the EU, private industry and charitable sources, and he holds several patents for instrumentation systems for monitoring in industry using optical techniques. He is extensively involved with the work of the professional bodies having been Chairman of the Science, Education and Technology of the Institution of Electrical Engineers (now IET), the Applied Optics Division of the Institute of Physics and was the President of the Institute of Measurement and Control during the year 2000. He has served on the Councils of all three of these Professional Bodies. He was awarded the Callendar Medal of the Institute of Measurement and Control in 1992, and twice the Honeywell Prize for work published in the Institute's journal as well as the Sir Harold Hartley Medal in 2012 for distinction in the field of instrumentation and control. He was awarded the Applied Optics Divisional Prize in 2010 for his work on optical sensing and the honorary degree of Doctor of the University of the University of Oradea in 2014. He was the elected President of the International Measurement Confederation (IMEKO) in 2014, serving from 2015 to 2018. He was elected to the Royal Academy of Engineering, the UK National Academy of Engineering, in 2008. He has been the Deputy Editor of the Journal Measurement Science and Technology for several years and currently serves on the Editorial Board of several major journals in his field in the USA and Europe. In January 2001, he was appointed as an Editor of the IMEKO Journal "measurement" and also serves on their General Council. He has been a member of the University Executive Committee (ExCo) since 2008 and chairs two of its sub-Committees; the University Sustainability Committee and the Business Continuity Management Committee. He has served on Senate for more than 20 years, as well as on many of its sub-Committees.

B. M. A. Rahman (Fellow, IEEE) received the B.S. and M.S. degrees from the Bangladesh University of Engineering and Technology, Dhaka, Bangladesh, in 1976 and 1979, respectively, and the Ph.D. degree from the University College London (UCL), London, U.K., in 1982. He joined City, University of London in 1988, got promoted to a Full professor in 2000 and has been serving there since then. He leads a research team of photonics simulation. He is a Fellow of OSA and SPIE.

Haimiao Zhou is currently working toward the master's degree in the major of optical engineering from Liaocheng University, Liaocheng, China.

Shien-Kuei Liaw (Senior Member, IEEE) received double Ph.D. degrees in photonics engineering and mechanical engineering from the National Chiao-Tung University, Hsinchu, Taiwan and National Taiwan University, Taipei, Taiwan in 2014. He joined the Chunghua Telecommunication, Taiwan, in 1993. Since then, he has been working on optical communication and fiber based technologies. He joined the Department of Electronic Engineering, National Taiwan University of Science and Technology (NTUST) in 2000. He has ever been the Director of the Optoelectronics Research Center and the Technology Transfer Center, NTUST. He was a Visiting Researcher with Bellcore (now Telcordia), USA for six months in 1996 and a Visiting Professor with the University of Oxford, U.K. for three months in 2011. He owned seven U.S. patents, and authored or coauthored for more than 250 journal articles and international conference presentations. He was the recipient of many national honors such as Outstanding Professor of the Chinese Institute of Electrical Engineering in 2015; the winner of The 7th Y. Z. Hsu Scientific Paper Award in 2009; the Best Project Award of National Science and Technology Program for Telecommunication in 2006; the outstanding Youth Award of The Chinese Institute of Electrical Engineering; and the outstanding Youth Academic Award of the Optical Engineering Society of the Republic of China. He has been actively contributing for numerous conferences as the Technical Program Chair, International Advisory Committee, Session Chair, Keynote Speaker, and Invited Speaker. He serves as an Associate Editor for *Fiber and Integrated Optics*. He is currently a senior member of OSA and SPIE. He is currently a Distinguished Professor and Vice Chairman of the ECE department, NTUST, Vice President of the Optical Society (OSA) Taiwan Chapter, and Secretary-General of Taiwan Photonic Society.

Chenglin Bai is a second-class Professor. He has authored more than 100 academic papers indexed by SCI and EI and has also authored monographs.

He was awarded the second prize of outstanding scientific research achievement award (science and technology progress award), two second prize of Shandong Science and Technology Award (natural science award), one third prize, and 2 third prize of Shandong Science and Technology Progress Award.